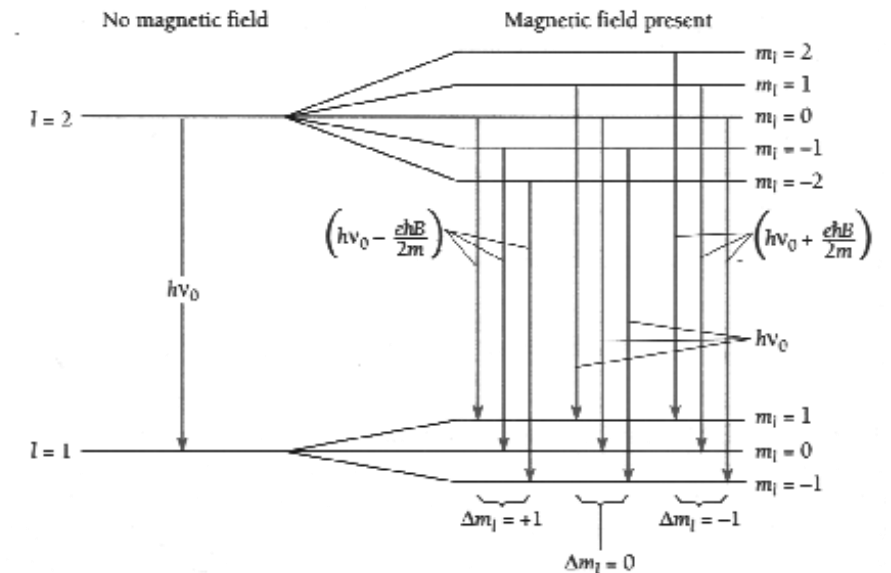
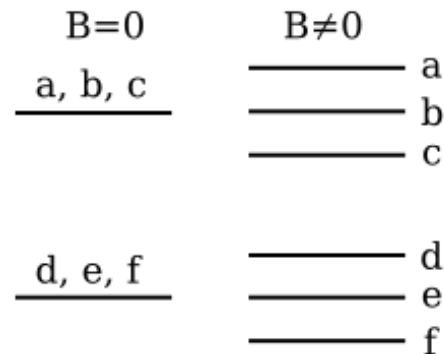
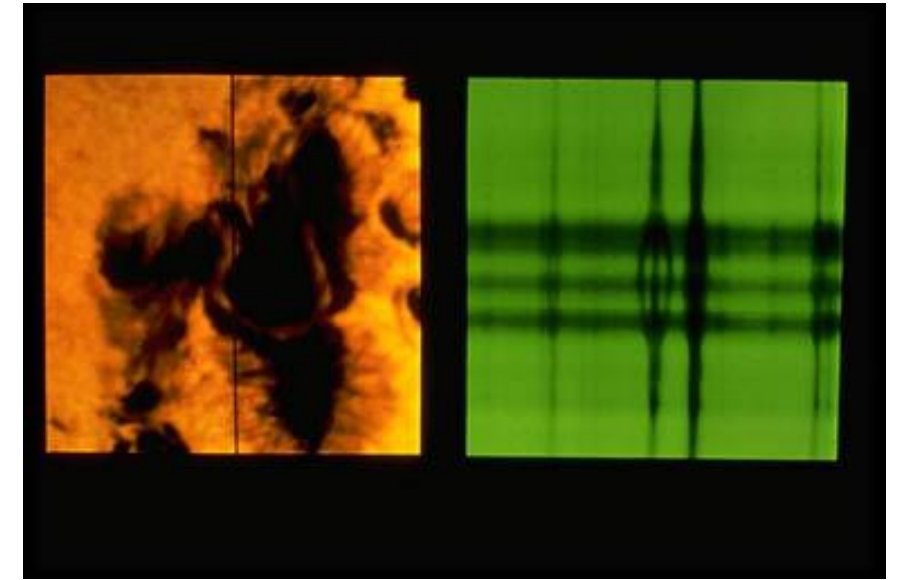
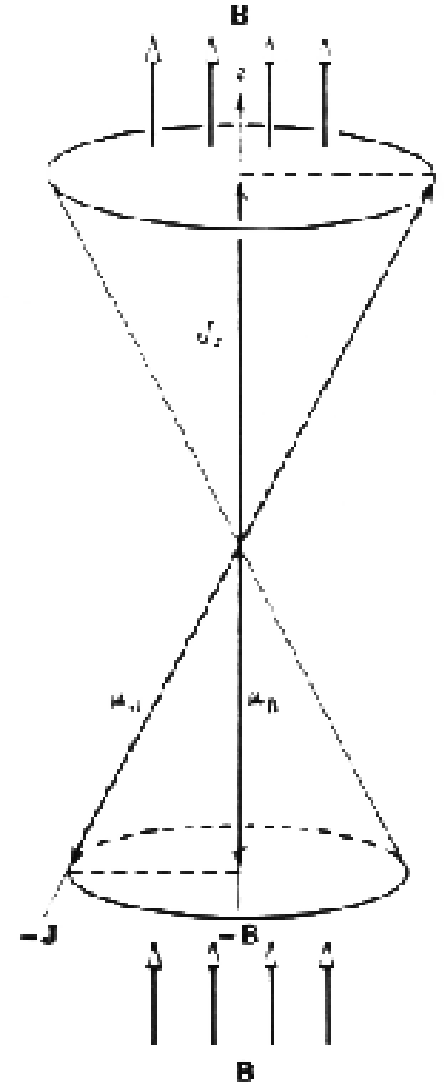
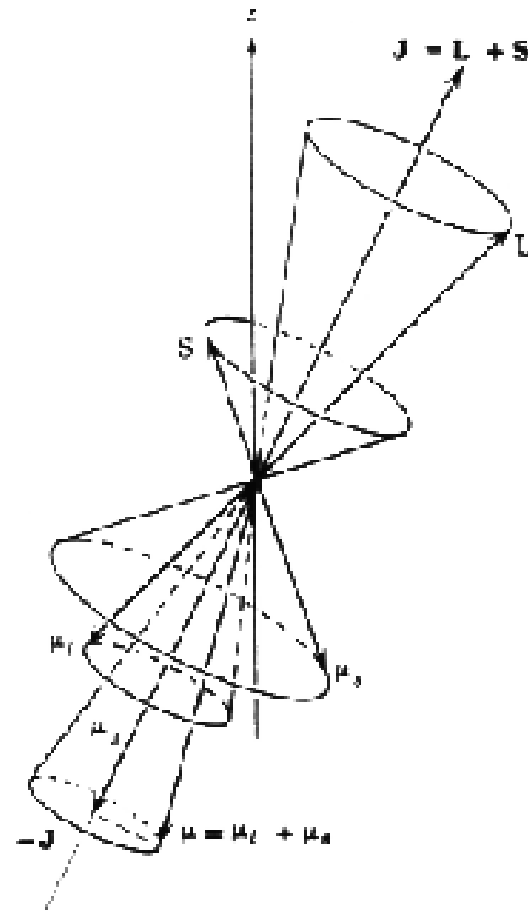


Zeeman Effect

... the split of a spectral line into several components in the presence of a **magnetic field**. It is analogous to the **Stark effect**, the splitting of a spectral line into several components in the presence of an **electric field**.

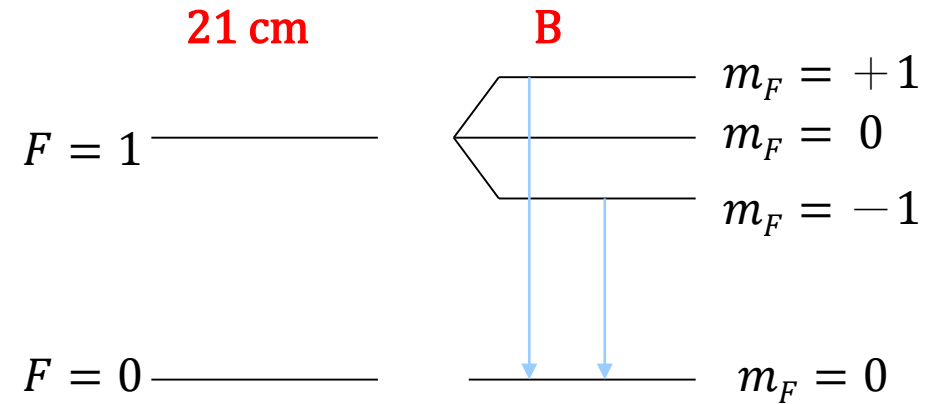




<http://www.pha.jhu.edu/~rt19/hydro/node10.html>

Selection Rule:

$\Delta m_F = 0, \pm 1$, but a level with $m_F = 0$ cannot combine with another $m_F = 0$



Singlet line $\rightarrow \sigma, \pi, \sigma$

$$-\frac{eB}{4\pi m_e c}$$

Elliptical
polarization

$$\nu_{mn}$$

Plane
polarization

$$+\frac{eB}{4\pi m_e c}$$

Elliptical
polarization

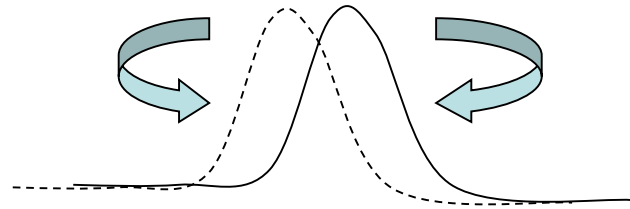
$$\frac{eB}{4\pi m_e c} = 1.4 \times 10^6 B_{\text{Gauss}} [\text{Hz}] \quad \text{Larmor frequency of precession}$$

Along \vec{B} , $\pi = 0$, σ s are circularly polarized in opposite directions

Total splitting $\Delta\nu = 2.80 \times 10^6 B_{\text{Gauss}} \text{ [Hz]}$

Typically in ISM, $B \sim 10^{-6} \text{ Gauss}$, so $\Delta\nu \sim$ a few hertzs

very difficult to detect (\ll Doppler width)



$$\langle B_{\text{Galactic}} \rangle \sim 4 \mu\text{G}$$

Zeeman splitting was first detected in 21-cm absorption (Verschuur 1969); later seen in emission, too (Heiles 1982)

Also has been observed in OH 18 cm line; 6 cm H_2CO

➔ to derive B and n (HI)

$B \propto n^\alpha$ for H I clouds, $\alpha \sim 2/3$ to $1/3$

Note: For an isotropically contracting cloud with a “frozen-in” magnetic field, $B \propto 1/R^2$, and because $\rho \propto 1/R^3 \Rightarrow B \propto n_H^{2/3}$

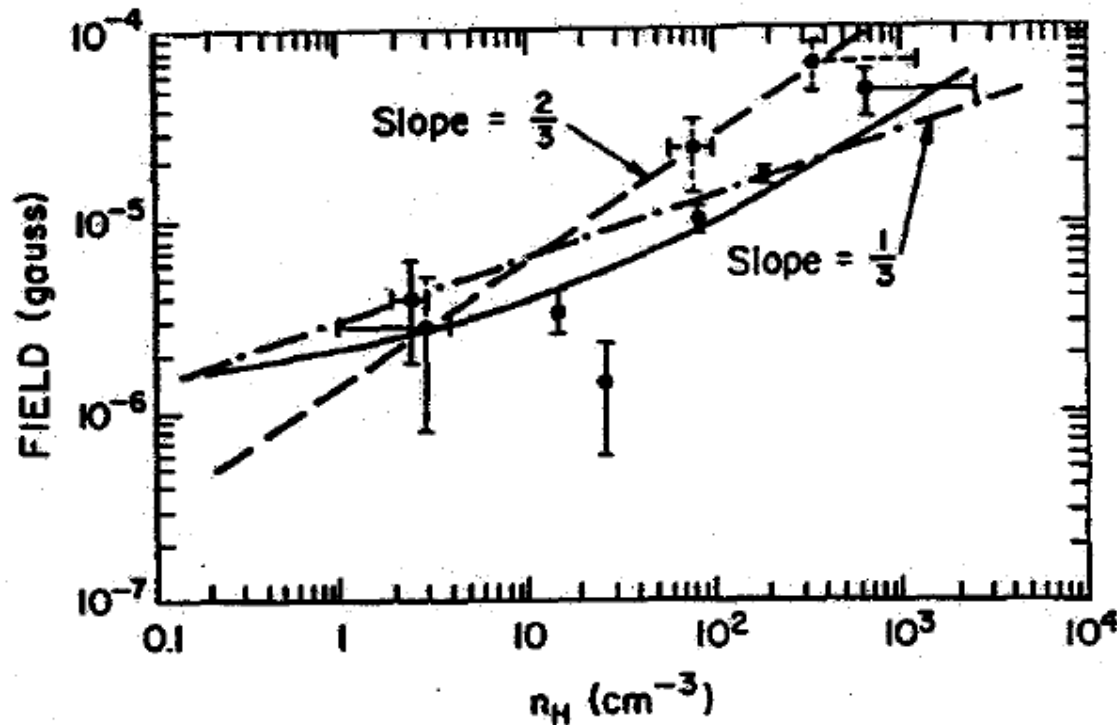


Fig. 1. Magnetic field strength in H I clouds as a function of gas density.

INTERSTELLAR MAGNETIC FIELD STRENGTHS AND GAS DENSITIES: OBSERVATIONAL
AND THEORETICAL PERSPECTIVES

T. H. TROLAND

Physics and Astronomy Department, University of Kentucky

AND

CARL HEILES

Astronomy Department, University of California, Berkeley

Received 1985 January 31, accepted 1985 July 16

ABSTRACT

We present an updated compilation of observational data concerning the relationship between the interstellar magnetic field strength and the gas density. Pulsar and Zeeman-effect data provide the only reliable information about the (B, n) relationship, and they now span nearly six orders of magnitude in gas density. Field strengths show no evidence of increase over the density range $0.1\text{--}\sim 100\text{ cm}^{-3}$. At higher densities, a modest increase in field strength is observed in some regions, in line with theoretical expectations for self-gravitating clouds. In two regions of the interstellar medium, the magnetic field is unusually high; however, these are not locales where self-gravitation is important. Despite the consistency between observations and theory, questions still exist about how the magnetic field strength remains constant for densities up to $\sim 100\text{ cm}^{-3}$. Further Zeeman effect studies and a better theoretical understanding of the formation of interstellar clouds and complexes will be necessary to answer these questions.

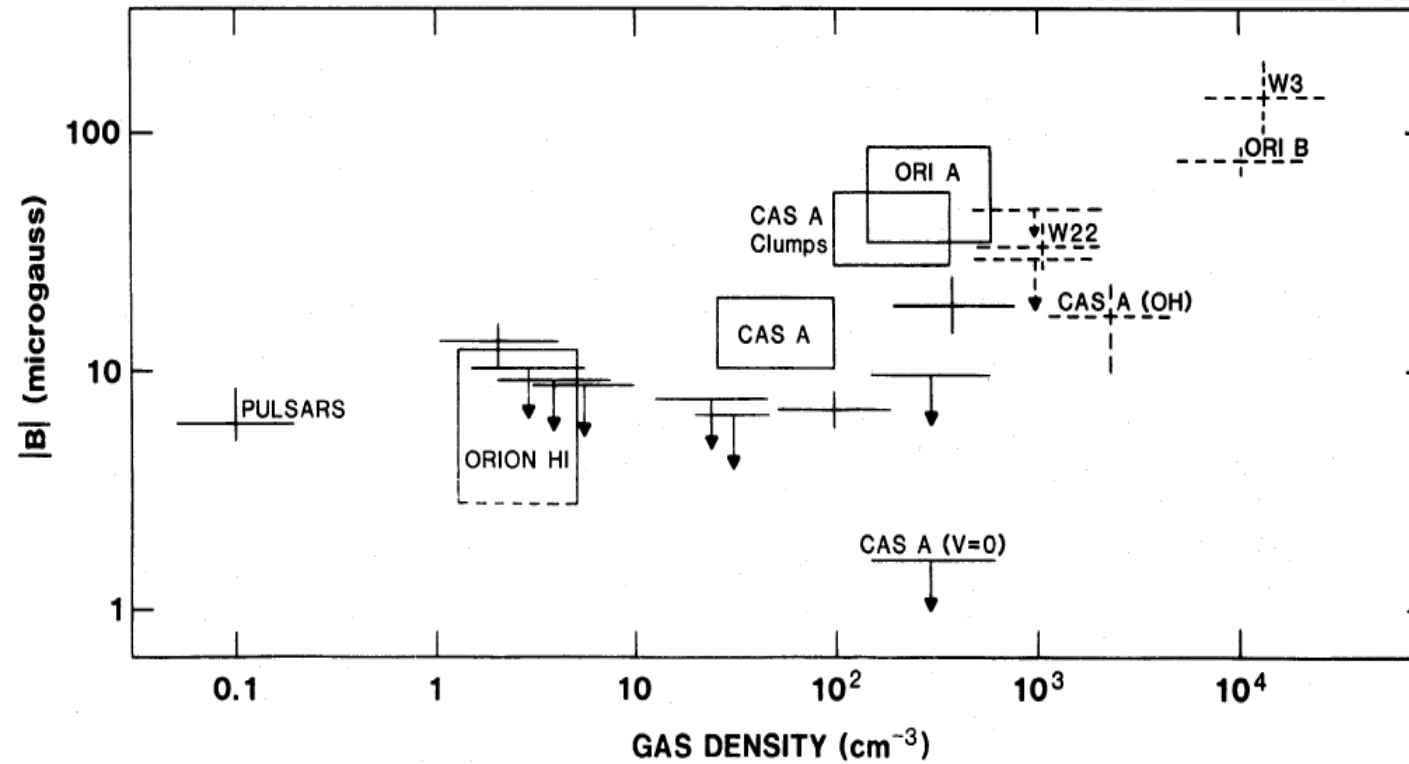


FIG. 1.—Observed magnetic field strengths as a function of estimated volume density. All results come from measurements of the H I (solid lines) and OH (dashed lines) Zeeman effect, except for the point labeled “pulsars.” This point is derived from pulsar rotation and dispersion measures. Rectangular boxes represent ranges of field strengths encountered in Zeeman effect maps made either with a single-dish or with aperture synthesis instruments. See § II for further details.

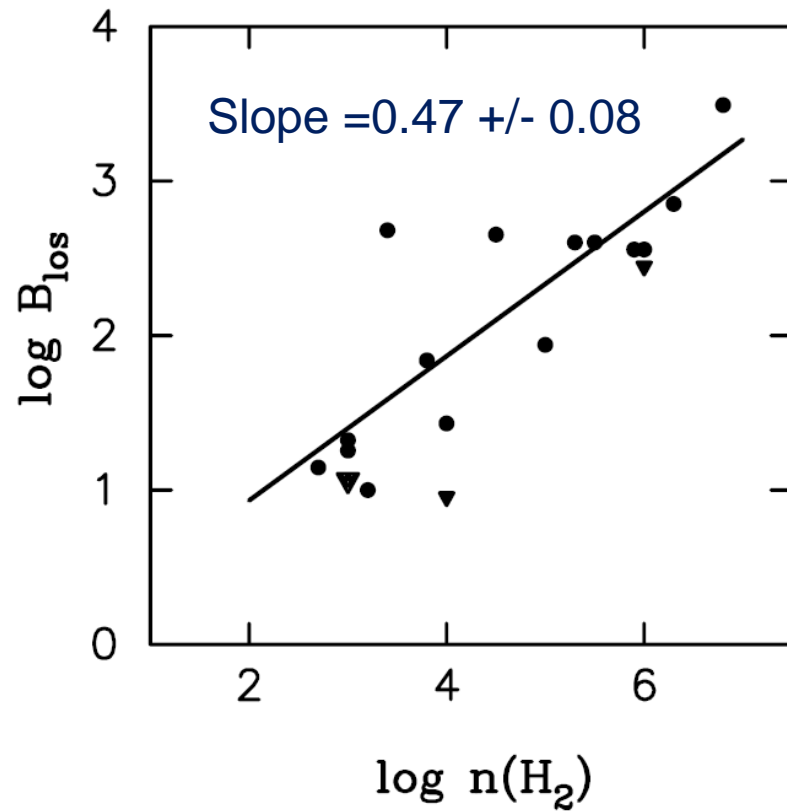


FIG. 1.—Plot of $\log B_{\text{los}}$ vs. $\log n(\text{H}_2)$. Inverted triangles are the upper limits for undetected clouds; the averaged limit for all of the dark clouds with $\log n(\text{H}_2) = 3$ is plotted as a single large inverted triangle. The line is the fit to detected clouds.

MAGNETIC FIELDS IN MOLECULAR CLOUDS: OBSERVATIONS CONFRONT THEORY

RICHARD M. CRUTCHER

Astronomy Department, University of Illinois, Urbana, IL 61801

Received 1998 November 16; accepted 1999 March 5

ABSTRACT

This paper presents a summary of all 27 available sensitive Zeeman measurements of magnetic field strengths in molecular clouds together with other relevant physical parameters. From these data input parameters to magnetic star formation theory are calculated, and predictions of theory are compared with observations. Results for this cloud sample are the following: (1) Internal motions are supersonic but approximately equal to the Alfvén speed, which suggests that supersonic motions are likely MHD waves. (2) The ratio of thermal to magnetic pressures $\beta_p \approx 0.04$, implying that magnetic fields are important in the physics of molecular clouds. (3) The mass-to-magnetic flux ratio is about twice critical, which suggests but does not require that static magnetic fields alone are insufficient to support clouds against gravity. (4) Kinetic and magnetic energies are approximately equal, which suggests that static magnetic fields and MHD waves are roughly equally important in cloud energetics. (5) Magnetic field strengths scale with gas densities as $|B| \propto \rho^\kappa$ with $\kappa \approx 0.47$; this agrees with the prediction of ambipolar diffusion driven star formation, but this scaling may also be predicted simply by Alfvénic motions. The measurements of magnetic field strengths in molecular clouds make it clear that magnetic fields are a crucial component of the physics governing cloud evolution and star formation.

Magnetic field strengths in galaxies determined by intensity of synchrotron emission, assuming equipartition between magnetic field and cosmic rays.

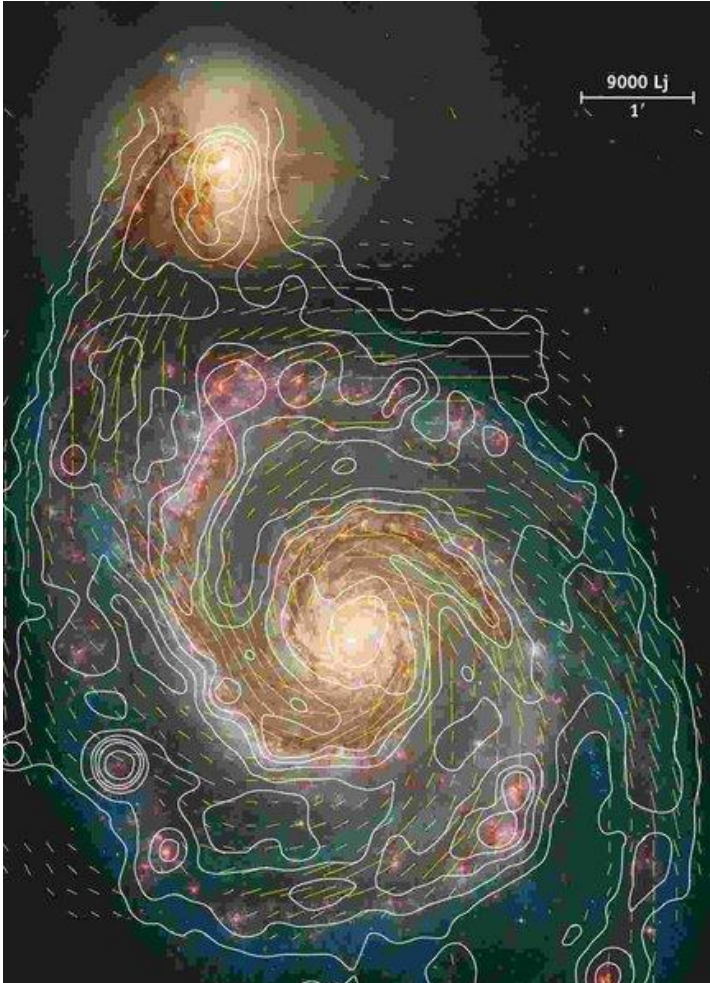
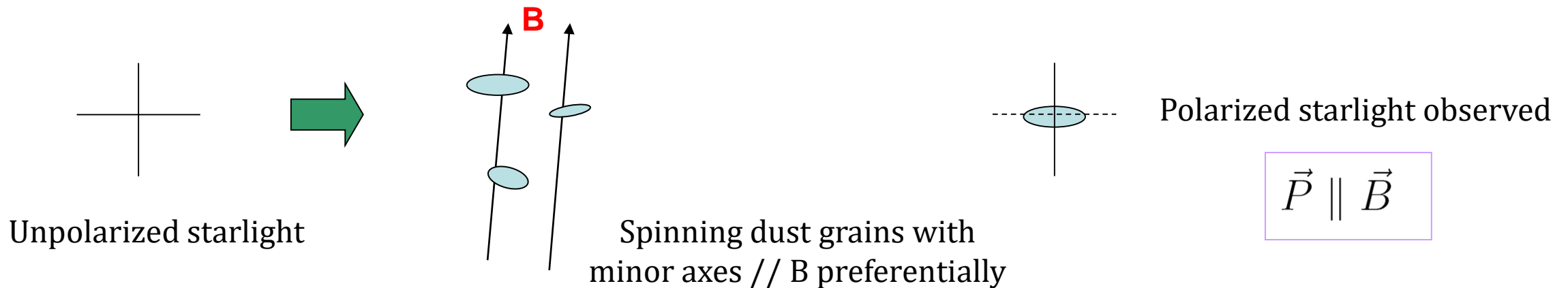


Figure 1: Optical image of the spiral galaxy M 51 obtained with the Hubble Space Telescope (from Hubble Heritage), overlaid by contours of the total radio intensity and polarization vectors at 6cm wavelength, combined from radio observations with the Effelsberg and VLA radio telescopes (from Fletcher and Beck, in prep.). The magnetic field follows well the optical spiral structure, but the regions between the spiral arms also contain strong and ordered fields. The bar in the top right corner indicates a scale of 1 arcminute or about 9000 light years (about 3 kiloparsecs) at the distance of the galaxy. Copyright: MPIfR Bonn

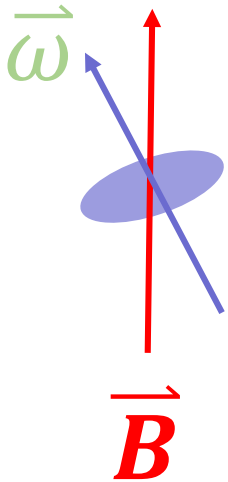
Polarized Starlight

Magnetic field in the ISM first discerned by linearly polarized starlight ($\sim 1\%$) (Hiltner 1949 and Hall 1949)

It is thought that the partial polarization of starlight is produced by elongated dust grains aligned by magnetic fields in the ISM (see a review by Lazarian astro-ph 0003314 “*Physics of Grain Alignment*”)



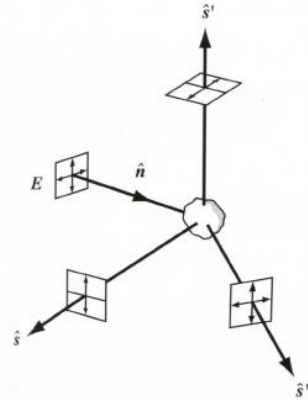
A thermalized ISM elongated grain tends to spin along its minor axis: $\vec{\omega} \rightarrow \vec{B}$



Davis-Greenstein
alignment mechanism
--- paramagnetic
dissipation

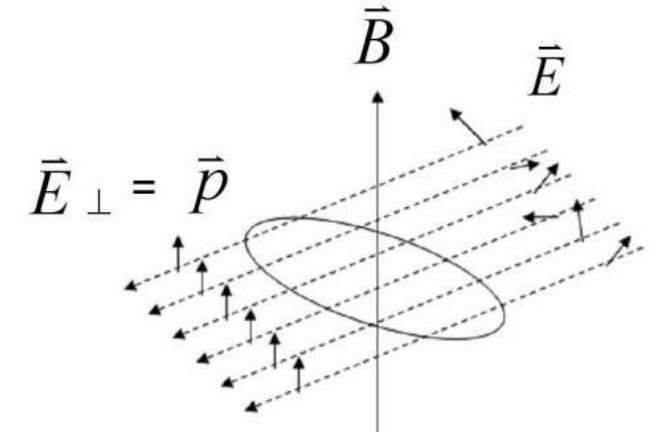
<http://bgandersson.net/grain-alignment>

Observations in OIR



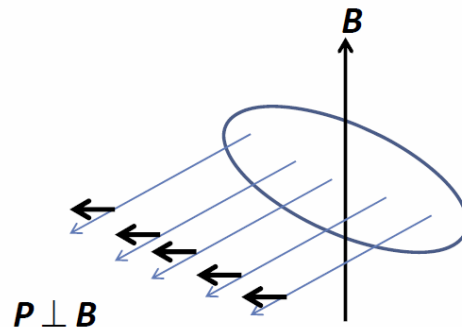
Stahler & Pallo 2004

Scattering by dust



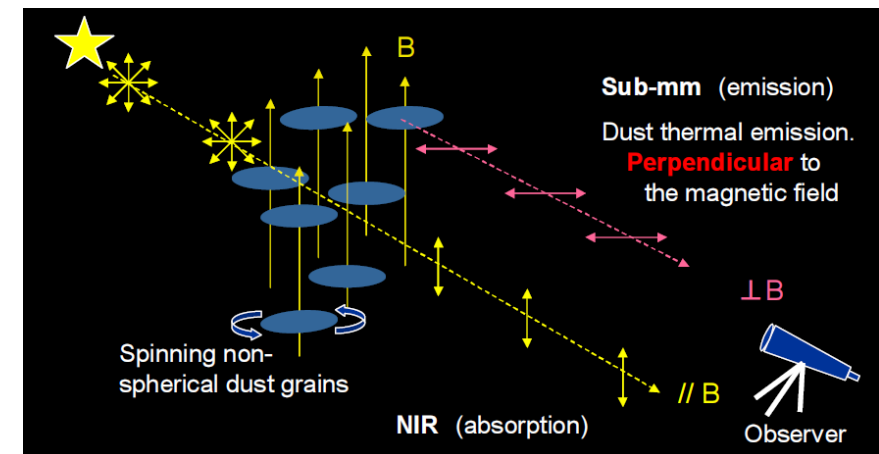
Dichroic extinction by aligned dust

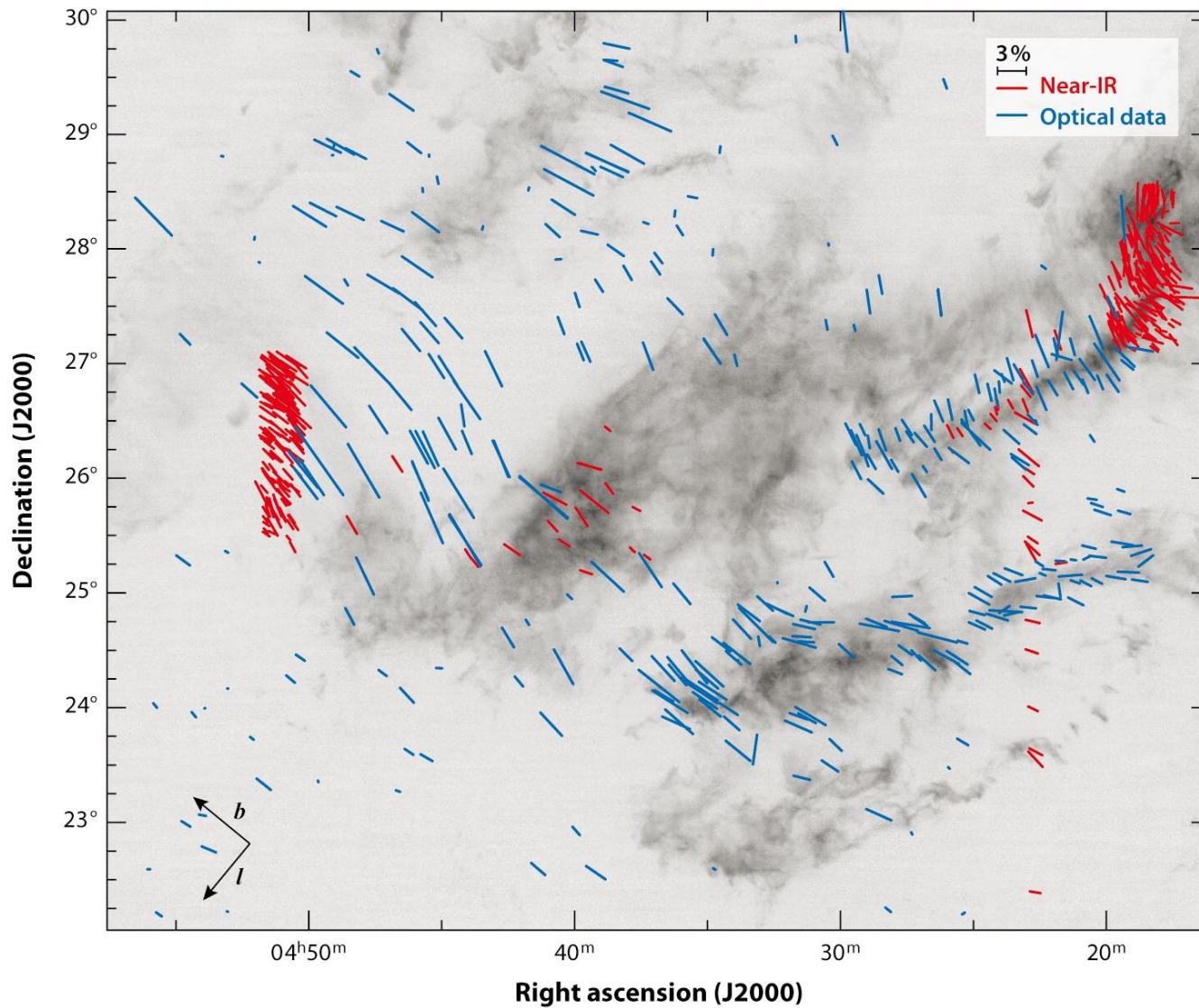
Observations in FIR to mm



*Polarized thermal emission by
dust aligned by B*

Courtesy: Tamura





Organized magnetic field morphology in the Taurus dark-cloud complex superposed on a ^{13}CO map (Chapman et al. 2011). **Blue** lines show polarization measured at optical wavelengths and **red** lines show near-IR (*H*-band and *I*-band) polarization.

Dichroic extinction by dust (optical and near-IR)

$$\vec{P} \parallel \vec{B}$$



Crutcher RM. 2012.

Annu. Rev. Astron. Astrophys. 50:29–63

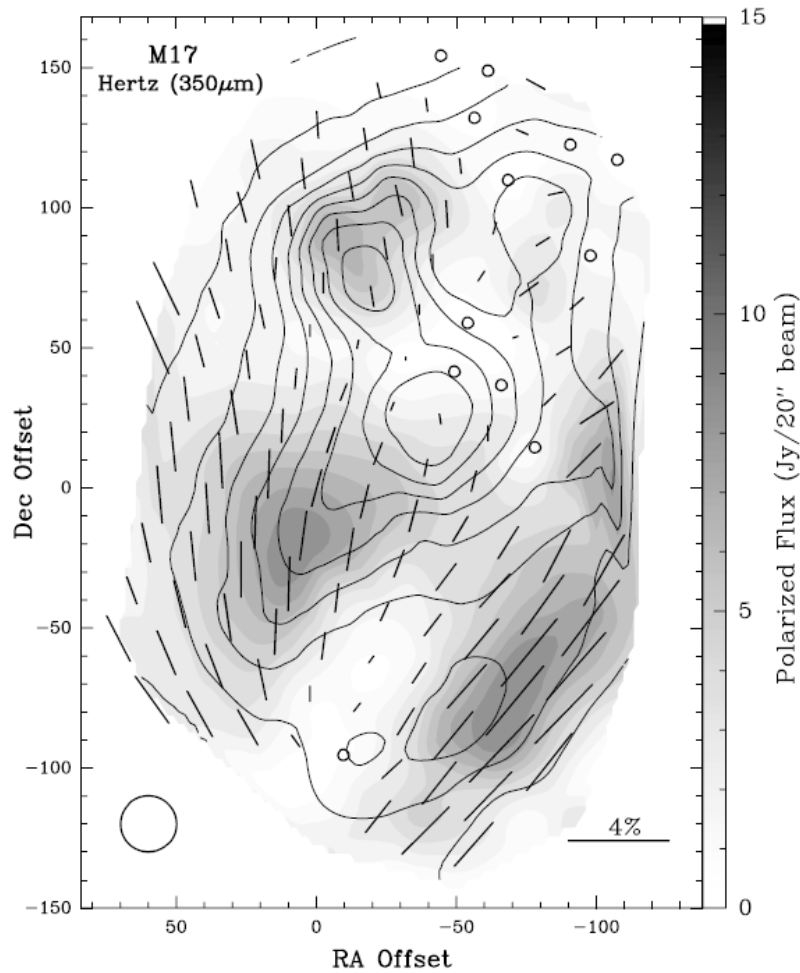


FIG. 6.—HERTZ polarization map of M17 at $350\ \mu\text{m}$. All of the polarization vectors shown have a polarization level and error such that $P > 3\sigma_p$. Circles indicate cases where $P + 2\sigma_p < 1\%$. The contours delineate the total continuum flux (from 10% to 90% with a maximum flux of $\approx 700\ \text{Jy}$), whereas the underlying gray scale gives the polarized flux according to the scale on the right. The beam width ($\approx 20''$) is shown in the lower left corner and the origin of the map is at R.A. = $18^{\text{h}}17^{\text{m}}31^{\text{s}}.4$, decl. = $-16^{\circ}14'25''.0$ (B1950.0).

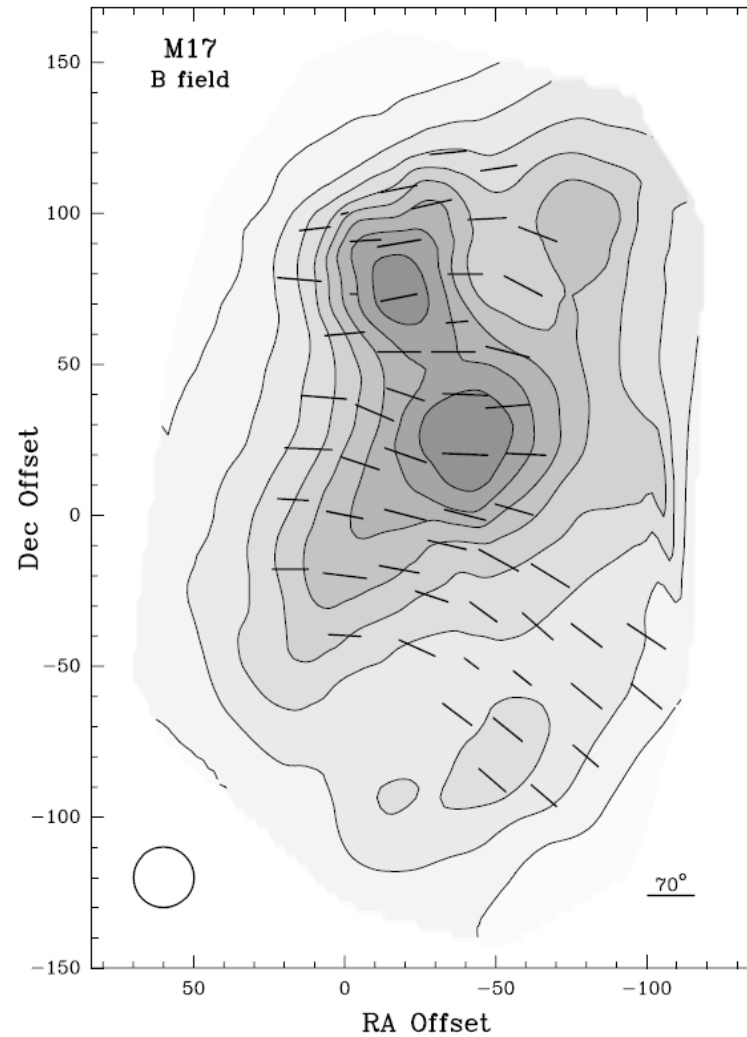


FIG. 11.—Orientation of the magnetic field in M17. The orientation of the projection of the magnetic field in the plane of the sky is shown by the vectors and the viewing angle is given by the length of the vectors (using the scale shown in the bottom right corner). The contours and the gray scale delineate the total continuum flux. The beam width ($\approx 20''$) is shown in the lower left corner, and the origin of the map is at R.A. = $18^{\text{h}}17^{\text{m}}31^{\text{s}}.4$, decl. = $-16^{\circ}14'25''.0$ (B1950.0).

Thermal emission
by dust (far-IR,
and smm)
 $\vec{P} \perp \vec{B}$

Houde et al. (2002)

Polarization of Light From Distant Stars by Interstellar Medium

W. A. Hiltner

Yerkes Observatory, University of Chicago

IN THE COURSE OF PHOTOELECTRIC OBSERVATIONS made last summer with the 82-inch telescope of the McDonald Observatory (University of Texas) the writer found that the light from distant galactic stars is polarized. Polarizations as high as 12 percent were found. The plane of polarization appears to be close to the galactic plane in the cases examined. More recently control measures were made at the Lick Observatory, thanks to the courtesy of Director Shane and Dr. G. Kron; and during December the work at the McDonald Observatory was extended to different regions of the Milky Way.

In view of the unexpected nature of this result the circumstances leading to its discovery are recorded. Photometric observations for the detection of partially polarized radiation from eclipsing binary stars have been in progress at the Yerkes Observatory for several years with a view to establishing observationally the effect pointed out by Chandrasekhar that the continuous radiation of early-type stars should be polarized (1, 2). On the assumption that the opacity of early-type stars is due to scattering by electrons, the continuous radiation emerging from a star should be polarized with a maximum of polarization of 11 percent at the limb. Since the presence of this polarization can be detected only when the early-type star is partially eclipsed by a larger-type companion of the system, the effect is masked by radiation from this companion so that the expected maximum observable effect was only of the order of 1.2 percent in one case investigated (RY Persei).

At this stage Dr. John Hall, of Amherst College, proposed to the writer a program of collaboration whereby Dr. Hall would construct a "flicker" photometer which was to be tested jointly at the McDonald Observatory. Independently the writer was developing his own equipment which used polaroids. Dr. Hall's equipment was tested in August 1947, during a short session at the McDonald Observatory, but no dependable results were obtained and it was found that the equipment had to be remodeled. Unfortun-

nately, Dr. Hall was unable to come for a second trial period, scheduled for August 1948.

Meanwhile the writer's own equipment was completed and put to use during the summer of 1948 and was found satisfactory. Certain Wolf Rayet stars which were known or suspected to be eclipsing binaries were examined for polarization. Fairly large polarizations were found, but *they did not appear to depend on the phase of the binary motion*. The possibility of instrumental polarization was considered, of course, but ruled out by control measures on check stars. The Wolf Rayet stars give the following results:

Star	Polarization	
	%	Position angle
CQ Cep	10.0	62°
BD 55°2721	8.0	44
WN Anon*	12.5	44

*Coordinates: 22°08' + 57°26' (1945); 12.5 magnitude.

The control stars had similar color and brightness, but showed no polarization except for one object, BD 55°2723, which gave 3 percent. This star, however, is a giant and more distant than the other control stars. Similar observations made on a group of Wolf Rayet stars in Cygnus showed no appreciable polarization, while two stars in Scutum gave positive results. Other regions, such as the double cluster in Perseus, also show polarization with values ranging up to 12 percent.

We conclude from the positive and negative results quoted that the measured polarization does not arise in the atmospheres of these stars but must have been introduced by the intervening interstellar medium. If this conclusion is accepted, a new factor in the study of interstellar clouds is introduced. Further observations are in progress for relating this phenomenon with other observable characteristics of interstellar medium. As has been stated, the results already at hand indicate that the plane of polarization approximates the plane of the galaxy.

References

1. CHANDRASEKHAR, S. *Astrophys. J.*, 1946, **103**, 365.
2. HILTNER, W. A. *Astrophys. J.*, 1947, **105**, 231.

Chandrasekhar
→ atmosphere of
early type stars
should produce
polarization due to
electron scattering

Polarization of
eclipsing binary WR
stars → polarization
does not change with
orbital phase

Polarization must
be of ISM origin

Pulsar Dispersion

Shape of the same pulse varies with freq.

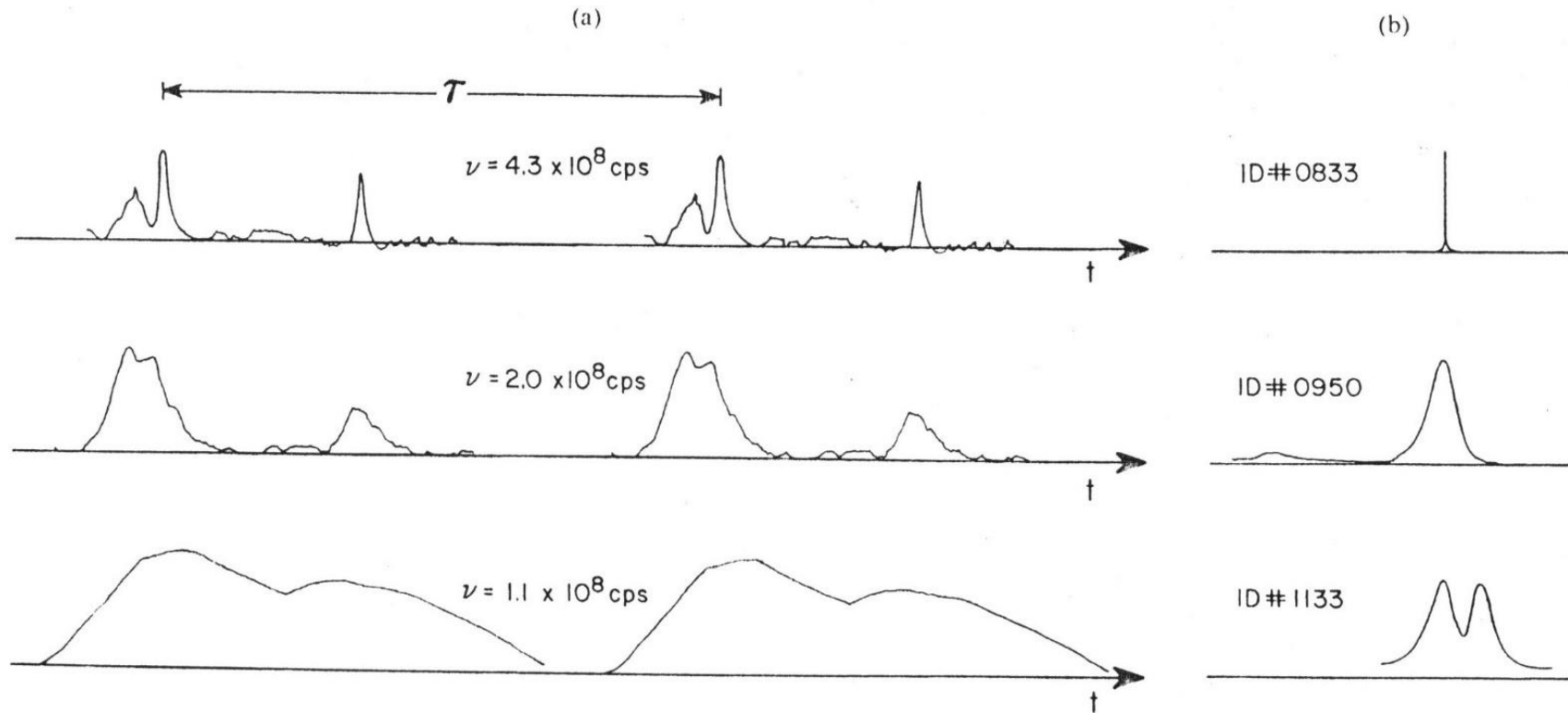
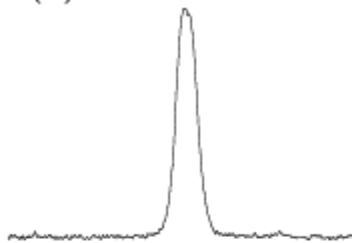


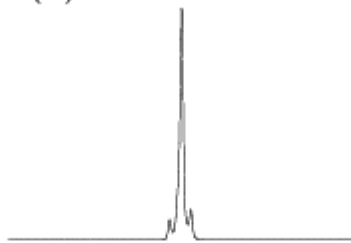
Fig. 5.8. Radio frequency detection of pulsars: (a) periodic pulse shape varying with frequency for a single pulsar; (b) integrated pulse shape for various pulsars.

Every pulsar is different.

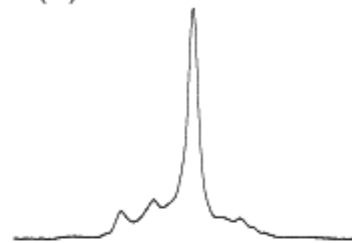
(a) B0031-07



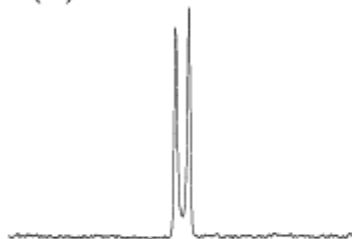
(b) B0329+54



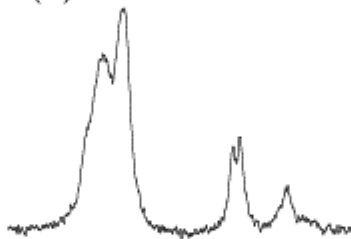
(c) J0437-4715



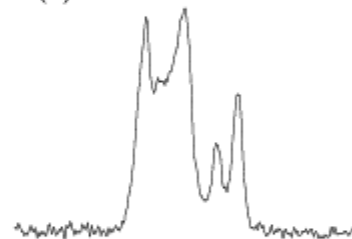
(d) B0525+21



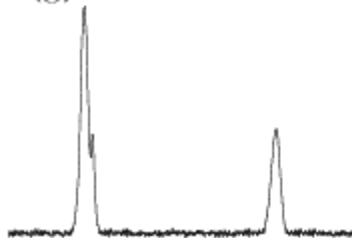
(e) J1012+5307



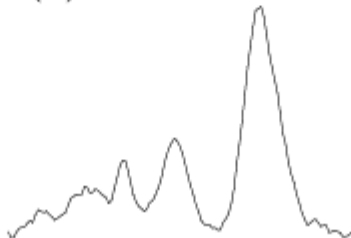
(f) B1831-04



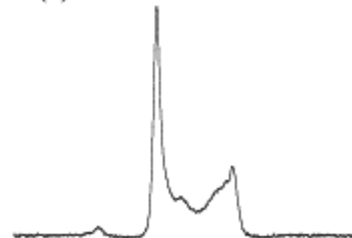
(g) B1937+21



(h) J2124-3358



(i) J2145-0750



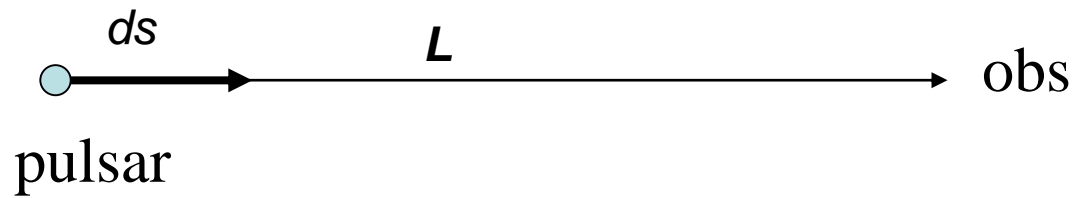
$$k = \frac{\omega}{v} = \frac{\omega}{c/n_r} \qquad n_r^2 = 1 - \frac{\omega_p^2}{\omega^2} \qquad \omega = \frac{k c}{n_r} = \frac{k c}{\sqrt{1 - \frac{\omega_p^2}{\omega^2}}}$$

$$\omega^2 - \omega_p^2 = k^2 c^2 \qquad 2\omega d\omega = 2k dk c^2$$

$$\frac{d\omega}{dk} = \frac{k c}{\omega} = c n_r = c \sqrt{1 - \frac{\omega_p^2}{\omega^2}}$$

Pulses propagate at the group velocity, which is frequency dependent.

$$v_{\text{group}} = \frac{d\omega}{dk} = c \left(1 - \frac{\omega_p^2}{\omega^2}\right)^{1/2}$$



Pulse traveling time = $\tau = \int_0^L \frac{ds}{v_g} = \int \frac{ds}{c(1 - \omega_p^2/\omega^2)^{1/2}}$

In ISM, $\omega^2 \gg \omega_p^2$, so $(1 - \omega_p^2/\omega^2)^{-1/2} \approx (1 + \omega_p^2/2\omega^2)$

$$\tau \approx \int_0^L \frac{ds}{c} (1 + \omega_p^2/2\omega^2)$$

Since $\omega_p = \sqrt{4\pi n e^2 / m}$, \longrightarrow $\tau \approx \frac{L}{c} + \frac{4\pi e^2}{2m\omega^2} \int_0^L n_e ds$

Traveling time \longleftrightarrow frequency

Signal arrives earlier at a higher frequency.

Dispersion Measure

(DM) [$\text{cm}^{-3} \text{ pc}$];

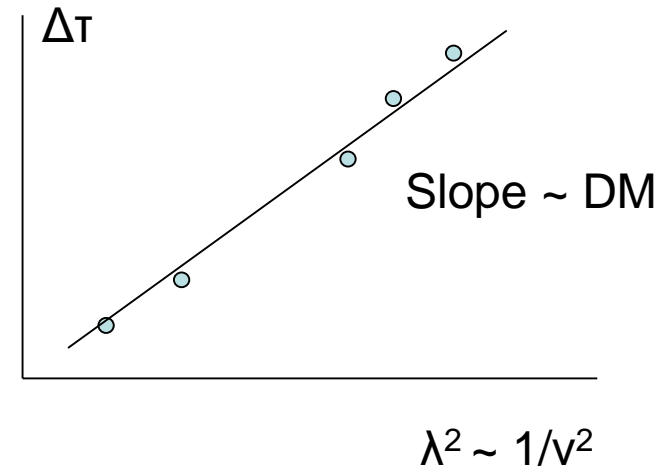
typical DM = 10 – 200

For ω_1 and ω_2 ,

$$\Delta\tau = \frac{4\pi e^2}{2m} \left(\frac{1}{\omega_1^2} - \frac{1}{\omega_2^2} \right) = 4.1 \times 10^3 \text{ DM} \left(\frac{1}{\nu_1^2} - \frac{1}{\nu_2^2} \right)$$

This gives DM $\rightarrow n_e$ along the line of sight in MHz

Observed $\langle n_e \rangle \sim 0.03$ to 0.08 cm^{-3}



Alternatively, one can assume n_e and estimate the distance.

In fact, n_e varies along the line of sight \rightarrow scintillation
(terrestrial 1", ISM 1 mas)

$ b $	< 2	2-5	5-10	10-30	30-90
DM	142	60	59	37	13

Dispersion measure of the ISM from observations of 60 pulsars for various intervals of Galactic latitude b (from Scheffler & Elsässer 1987 based on Pottasch 1974)

Faraday Rotation

What if there is magnetic field?

The effect in which the plane of polarization of an EM wave is rotated under the influence of a magnetic field parallel to the direction of propagation

$$n_r^2 = 1 - \omega_p^2/\omega^2 \text{ is modified, } \longrightarrow \boxed{n_r^2 = 1 - \frac{\omega_p^2}{\omega(\omega \pm \omega_B)}}$$

$$\text{where } \omega_B = \frac{eB}{mc} = \frac{4.8 \times 10^{-10} \times 10^{-6}}{10^{-27} \times 3 \times 10^{10}} \sim 10 \text{ [Hz]}$$

$B \rightarrow$ different $n_r \rightarrow$ different phase velocities for 2 opposite circular polarizations (linear polarization with a specific position angle) \rightarrow PA rotates

$$\text{In ISM, } \omega (\sim 10^8 \text{ Hz}) \gg \omega_p (\sim 10^4 \text{ Hz}) \gg \omega_B (\sim 10 \text{ Hz})$$

$$\frac{\omega_p^2}{\omega^2(1 \pm \omega_B/\omega)} \approx \frac{\omega_p^2}{\omega^2}(1 \mp \omega_B/\omega)$$

$$n_r^2 = 1 - \frac{\omega_p^2}{\omega^2} \pm \frac{\omega_p^2 \omega_B}{\omega^3}$$

original
change

$$n_r = \left(1 - \frac{\omega_p^2}{\omega^2} \pm \frac{\omega_p^2 \omega_B}{\omega^3}\right)^{1/2} \approx \left(1 - \frac{\omega_p^2}{\omega^2} \pm \frac{\omega_p^2 \omega_B}{2\omega^3}\right) \equiv n_{r,0} \pm \Delta n_r$$

$$\begin{aligned} \text{Phase} &= \varphi = k n_r \mathfrak{z} = \frac{\omega}{c} \frac{\omega_p^2 \omega_B}{2\omega^3} \mathfrak{z} \\ &= \frac{\lambda^2}{8\pi^2 c^3} \frac{4\pi e^2}{m} \frac{e}{mc} \int B n ds \\ &\equiv \lambda^2 RM \end{aligned}$$

Rotation Measure

$$RM = \frac{e^3}{2\pi m^2 c^4} \int n_e B_{\parallel} ds = 8.12 \times 10^5 \int_0^L n_e B_{\parallel} ds$$

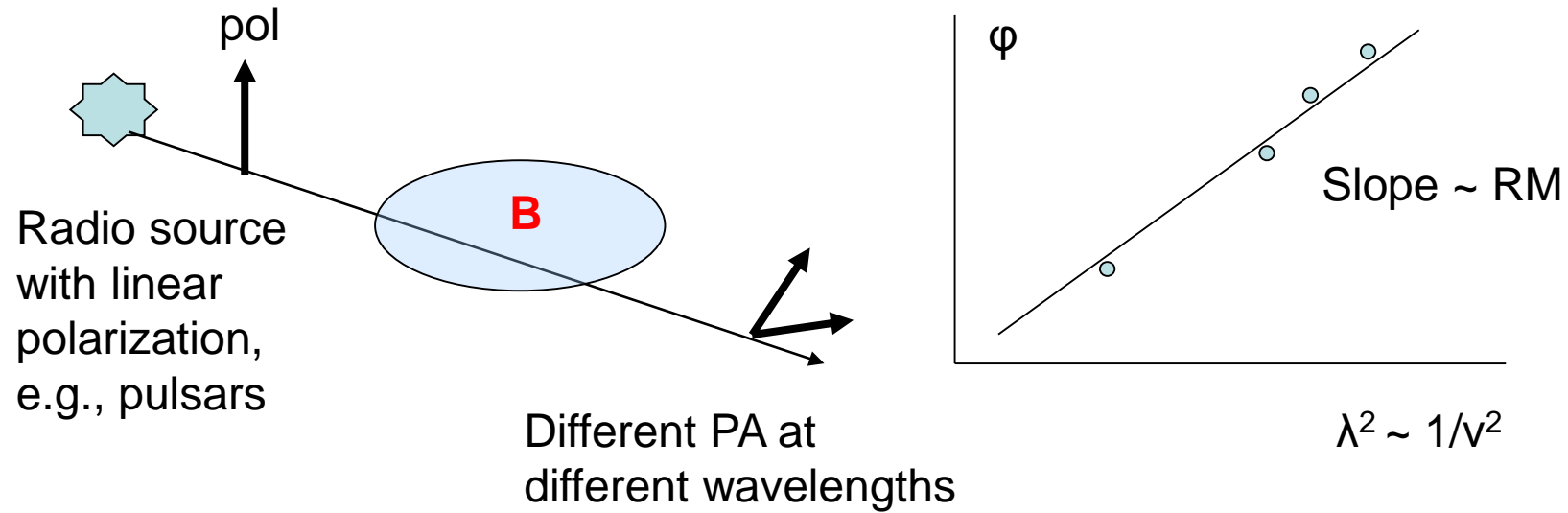
ds [pc]; n_e [cm⁻³]; B [Gauss]; λ [m]; ϕ [radian]

Note:

$$EM = \int n_e^2 ds$$

$$DM = \int n_e ds$$

$$RM = \int n_e B_{\parallel} ds$$

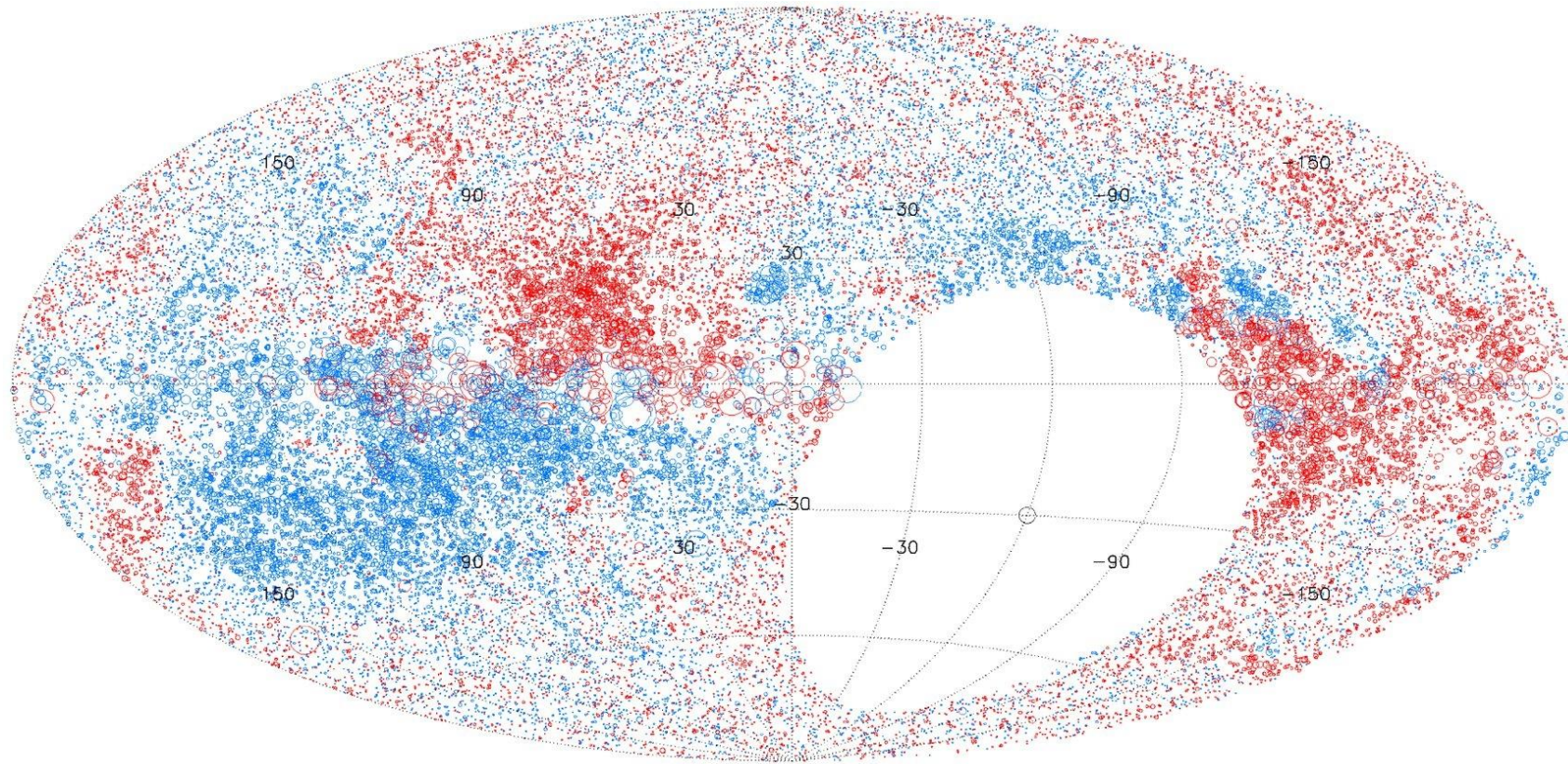


For polarized pulsars for which DMs are known

$$\frac{\int n_e B_{\parallel} ds}{\int n_e ds} = \frac{1}{8.1 \times 10^5} \frac{RM}{DM} = \langle B_{\parallel} \rangle$$

e.g., $B(\text{Vela}) \sim 0.8 \mu\text{G}$

For galaxies, guess n_e and get B



Plot of 37,543 RM values over the sky north of $\delta = -40^\circ$. Red circles are positive rotation measure and blue circles are negative. The size of each circle scales linearly with magnitude of rotation measure. (Taylor et al. 2009 ApJ, 702, 1230)